HOSTED BY

ELSEVIER

Available online at www.sciencedirect.com

ScienceDirect

Progress in Natural Science: Materials International 25 (2015) 197–203

Progress in Natural Science Materials International

www.elsevier.com/locate/pnsmi
www.sciencedirect.com

Original Research

In vitro and *in vivo* investigation of bacterial cellulose dressing containing uniform silver sulfadiazine nanoparticles for burn wound healing

Xiaoxiao Wen[a], Yudong Zheng[a,*], Jian Wu[b], Lina Yue[a], Cai Wang[a], Jiabin Luan[a], Zhigu Wu[c], Kaisheng Wang[a]

[a]*School of Materials Science and Engineering, University of Science and Technology Beijing, Beijing 100083, China*
[b]*Suzhou Institute of Nano-Tech and Nano-biobics, Chinese Academy of Sciences, Soochow 215123, China*
[c]*Hospital Affiliated to Chinese PLA General Hospital, Beijing 100853, China*

Received 13 March 2015; accepted 23 April 2015
Available online 8 July 2015

Abstract

Silver sulfadiazine (SSD) particles in homogeneous dispersion state were prepared by an ultrasonic method and then nano- and microparticles were separated using centrifugation. SSD particles with narrow size distribution were impregnated with bacterial cellulose (BC) to produce BC–SSD composite membrane used as burn wound dressing. A scanning electron microscope (SEM) was used to examine the surface morphology of BC–SSD membranes. The incorporation of SSD in BC–SSD was confirmed by X-ray diffraction (XRD). Antimicrobial tests *in vitro* indicated that BC–SSD showed excellent antibacterial activity against *Staphylococcus aureus*, *Pseudomonas aeruginosa* and *Escherichia coli*. The effects of BC–SSD on burn wound healing were assessed by rat models. The comparative study confirmed that the wound treated with BC–SSD showed high healing rate. The bacteria count in BC–SSD group was far less than control group. Histological analysis showed that epithelialization progressed better in wound treated with BC–SSD. These values demonstrated that the BC–SSD composite membrane could be a promising wound dressing for burn.

Keywords: Bacterial cellulose; Silver sulfadiazine; Antibacterial activity; Burn wound healing

1. Introduction

Every year, numerous patients suffer from burns due to various accidents [1]. The problems associated with burns treatment remain a clinical challenge. A large number of dressings have emerged with a variety of options for burn wound management [2]. An ideal burn wound dressing should have a lot of key attributes, such as the ability to prevent bacterial infections, provision of an optimal moist environment, favorable biocompatibility and cost saving [3,4].

Bacterial cellulose (BC) is a biosynthetic cellulose produced by strains of the Gram-negative bacterium *Acetobacter xylinum* using glucoses as the common substrate [5,6]. BC displays high purity, tensile strength, water holding capacity, and biocompatibility, and has a unique nanofibril network morphology which mimics the extracellular matrix [7,8]. Due to these special properties, BC has gained particular interest recently in biomedical applications, such as drug-delivery application [9], vascular [10] and blood vessels [11,12] graft, scaffolds for bone [13] and cartilage [14] tissue engineering, wound dressing [15,16] and skin repair [17]. Among them, wound dressing is one of BC's best known biomedical applications since BC can control wound exudates and provide moisture environment, which has been shown to accelerate wound healing [7,18]. However, BC do not have inherent antibacterial property and thus lack of ability to prevent bacteria infections in wound. For this reason, microorganism pollution is a major concern for BC applications [19,20]. To solve this problem, several studies have added silver and silver compounds as antibacterial into BC, and this approach has

*Corresponding author. Tel.: +86 10 62330802.
E-mail address: zhengyudong@mater.ustb.edu.cn (Y. Zheng).
Peer review under responsibility of Chinese Materials Research Society.

http://dx.doi.org/10.1016/j.pnsc.2015.05.004

yielded some success in antibacterial action and burn wound healing [21–24].

Silver sulfadiazine (SSD) has been widely used as an antibacterial agent for topical treatment of burn wounds for several decades [25,26]. It has remarkable broad-spectrum antimicrobial activities and improved burned patient survival [4,27]. Previously, our group has studied the optimal conditions for preparation of SSD particles-impregnated BC membrane (BC–SSD), which has been proved to exhibit strong antimicrobial activity against *P. aeruginosa*, *E. coli* and *S. aureus* and show favorable biocompatibility [28]. To further investigate the effect of the BC–SSD membranes as wound dressing on the burn healing process, we performed *in vivo* experiments in rat models to compare BC–SSD with gauze in wound healing. From previous study, we found that large SSD particles with very wide size distribution were formed in non-dispersed suspension, while small particles with narrow size distribution were more likely to deeply penetrate into bacterial cellulose. As a follow up study, we used a centrifugation method to better separate different sizes of SSD particles after ultrasonication. The suspended particles (SSD-s) and precipitation (SSD-p) were collected separatly to composite with BC. The structures of BC–SSD-s and BC–SSD-p membranes were compared by SEM and XRD. The antibacterial activity of BC–SSD-s and BC–SSD-p against *P. aeruginosa*, *E. coli* and *S. aureus* were characterized by by disc diffusion and a shake flask test method *in vitro*. Finally, BC–SSD-s membranes were selected and then evaluated in the rat model, influence of BC–SSD-s on anti-infection and concrescence in partial thickness burn wound model were studied in details.

2. Materials and methods

2.1. Preparation of SSD particles

SSD suspension (2 wt%, pH = 7.0) in distilled water was dispersed by a ultrasonic cell pulverizer (SCIENTZ, JY92-II, China) for 90 min to achieve SSD particles. Then the suspended particles were centrifugated for another 30 min at 3000 rpm. The suspended particles and precipitation were collected separately. The diameter of SSD particles was determined by a particle analyzer (Beckman Colter, DelsaTM Nano C, USA).

2.2. Impregnation of SSD into BC

BC membranes (Hainan Yida Food Co. Ltd, China) were purified as previous study [28]. Briefly, BC were immersed in 0.1 M NaOH aqueous solution at 90 °C for 60 min, then rinsed with deionized water. BC membranes were soaked in supernatant and precipitation of SSD separately for 24 h, the obtained samples were dried at room temperature to remove excess moisture.

2.3. Characterization of BC–SSD composite membrane

2.3.1. SEM analysis

Samples were freeze-dried in a Vacuum Freeze Dryer at −50 °C. Then gold was sputtered on samples to improve contrast. SEM pictures were taken at different magnifications with SEM (Carl Zeiss, AURIGA Cross Beam FIB/SEM station, Germany).

2.3.2. X-ray diffraction

Crystal structure of BC–SSD was studied by a X-ray diffractometer (Rigaku Corporation, Japan). The samples were scanned from 10° to 70° with the speed of 10°/min.

2.4. Antimicrobial activity of BC–SSD membrane

The antibacterial activity of BC–SSD membrane was studied against *P. aeruginosa* (ATCC10211), *E. coli* (ATCC44113) and *S. aureus* (ATCC26085) using two methods as previous study [28]. Gauze and a commercial silver-containing dressing (Coloplast® Ag nonadhesive foam dressing) were setted as negative and positive control, respectively. *S. Aureus*, *E. Coli* and *P. Aeruginosa* were cultured for 24 h in *Staphylococcus* medium, eosin-methylene blue medium and blood agar medium, respectively, and then culture solution was diluted with sterile saline solution to a concentration of 1×105 CFU/mL. In the disk diffusion method, samples were cut into circular discs (6 mm in diameter), sterilized by autoclaving 20 min at 120 °C and pressed into the bacteria-seeded agar plates (8 per plate) which was then incubated for 24 h at 37 °C and the inhibition zone was monitored. In the shake flask test method, the samples (0.4 g) were placed in shaking flasks and inoculated with 2.5 ml of bacterial inoculums. The flasks were then shaken for 24 h at 37 °C. The number of bacteria was obtained by spread plating serial dilutions on nutrient agar. The reduction percentage in bacterial count and bacteriostatic rate were determined using the following formula:

$$\text{Bacteriostatic rate}(\%) = (B-A)/B \times 100$$

Where A is colony forming unit counts/mL (CFU/mL) of the samples at 24 h; B is CFU/mL of the negative control at 24 h.

2.5. In vivo burn wound healing

2.5.1. In vivo experiment

Wistar rats (250 g approximately) were used in this study. All handling and maintenance were in accordance to institutional ethical use protocols. After anesthetizing with 45 mg $kg-1$ pentobarbital sodium, the animals were locally shaved and disinfected using 75% ethanol. Partial thickness skin wounds (20 mm × 20 mm) were made on the back region with scald apparatus at 60 °C for 20 s. The wounds were covered with BC–SSD-s membranes and gauze as control group. At 4, 7, 10 and 14 days after post-surgery, the rats were euthanised in accordance with ethical standards, and changes in the wounds were evaluated macroscopically, histopathologically, and microbiologically in all groups.

2.5.2. Wound healing rate

At 4, 7, 10 and 14 days post-surgery, the wound size measurement was taken by measuring the photographs of the

wounds with the software Image-Pro plus 6.0. The wound healing rate was defined as [29]:

$$\text{Wound healingrate}(\%) = (A_0 - A_t)/A_0 \times 100$$

where $A0$ and At denote initial wound area and wound area after time interval "t", respectively.

2.5.3. Bacteria count

At defined timepoints, a sterile filter paper was used to swab in the wound bed rotating clockwise for 30 s three times. Filter papers were placed into a tube; homogenized in 1 mL of sterile saline; and plated serially on agar plates to assess the bacterial counts.

2.5.4. Histology

Biopsies were obtained from the wound area and fixed in formalin. Samples were embedded in paraffin and stained with hematoxylin and eosin (H&E) or Masson's trichrome. The measurements of the thickness of the epidermis and dermis were based on those made from H&E-stained tissue sections using image analyzing software (Olympus Cellsens Entry software, Tokyo, Japan).

2.6. Statistical analyses

Statistical analysis of data was performed by one-way analysis of variance (ANOVA), assuming confidence level of 95% ($P < 0.05$) for statistical significance. All the data were expressed as mean ± standard deviation (SD).

3. Results

3.1. Particle size of SSD

Fig. 1 showed the different particle size distributions of SSD. SSD particles without sonication and centrifugation showed large particles with a wide distribution. The particle diameter of SSD particles after sonication and centrifugation decreased. The supernatant (SSD-s) and precipitation (SSD-p) of SSD particles after centrifugation displayed average particle size of 282.3 ± 22.7 nm and 2149.5 ± 173.6 nm, respectively with a progressively narrow distribution of particle sizes. We assumed that SSD-s was more suitable to composite with BC, as the average diameter of holes in BC was approximately hundreds of nanometers.

3.2. Structure of BC-SSD

3.2.1. Morphology of BC and BC-SSD

Fig. 2 shows the SEM micrographs of BC and BC-SSD in different magnifications. As shown in Fig. 2-D, BC had a fibrous network with highly porous structure. At low magnification, SSD particles attached on the BC in both BC–SSD-s and BC-SSD-p composite membrane. At high magnification (Fig. 2(A)–(C)), it is showed that the network of BC was well retained after impregnation of SSD into BC (Fig. 2(E) and (F)). Furthermore, BC–SSD-s composite membrane showed smaller and fewer SSD particles attached compared with BC–SSD-p composite membrane, which were well dispersed in the inner fibers of BC.

3.2.2. Crystal structure of BC and BC–SSD

In order to examine the crystallographic structure, BC, SSD and BC–SSD were analyzed using XRD (Fig. 3). For original BC, characteristic peaks at 14.8°, 16.3° and 22.6° was observed, which correspond to the crystal planes as (1–10), (110), and (200). For SSD, its characteristic peaks located at 8.8°, 10.21° and 18.49° corresponding to (002), (011) and (020) planes. In BC–SSD-p and BC–SSD-s, the characteristic peaks of BC remained the same, implying that the size of SSD particles had no effects on the crystal structure of BC. The intensity of characteristic peaks of SSD at 10.21° and 18.49° in BC–SSD-p was higher than that in BC–SSD-s, as the evidence of the more SSD content in BC–SSD-p compared in BC–SSD-s.

3.3. Antimicrobial activity of BC–SSD

The antimicrobial activity of BC–SSD against *S. aureus, E. coli and P. aeruginosa* was measured by the disc diffusion method (Fig. 4). In every test, both BC–SSD-s and BC–SSD-p exhibited obvious inhibition zone while no inhibition zone was observed for the gauze. BC–SSD-p composite membrane showed larger inhibition zone than BC–SSD-s composite

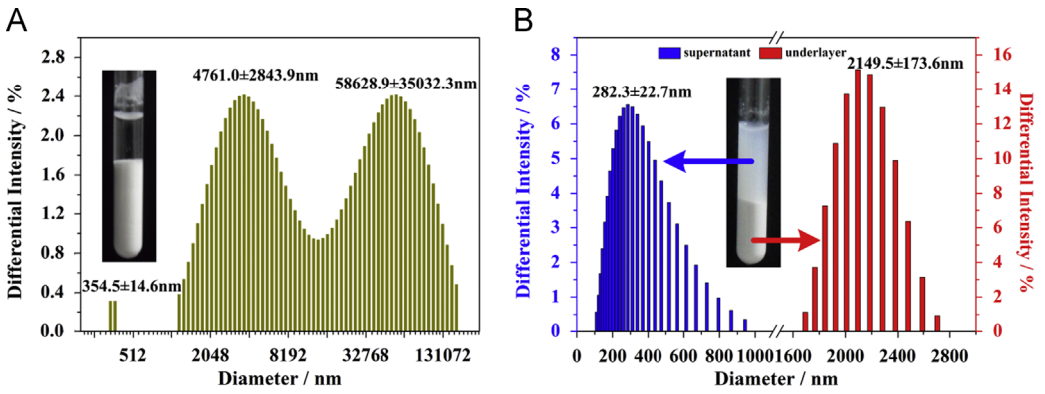

Fig. 1. Particle size distribution of (A) SSD particles without ultrasonication and centrifugation, (B) supernatant (SSD-s) and precipitation (SSD-p) of SSD particles after ultrasonication and centrifugation.

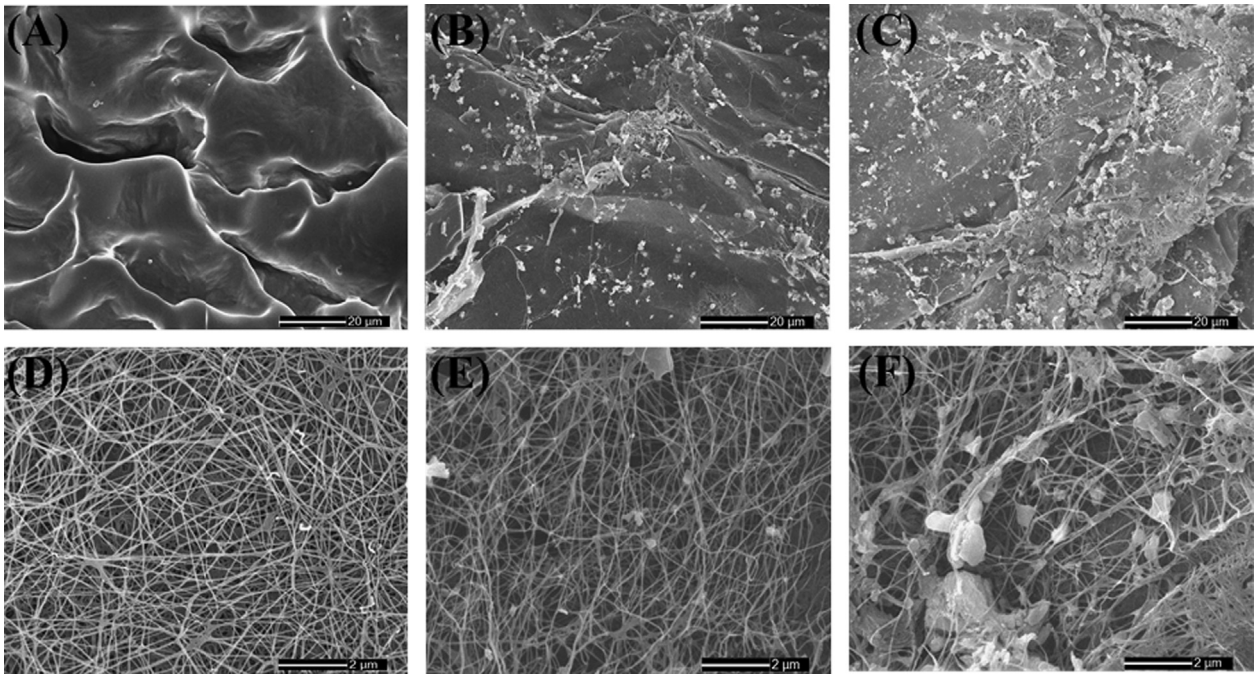

Fig. 2. Scanning electron microscopy morphology of (A) Bacterial Cellulose (2000 ×); (B) BC–SSD-s composite membrane (2000 ×); (C) BC–SSD-p composite membrane (2000 ×); (D) Bacterial Cellulose (20,000 ×); (E) BC–SSD-s composite membrane (20,000 ×); (F) BC–SSD-p composite membrane (20,000 ×).

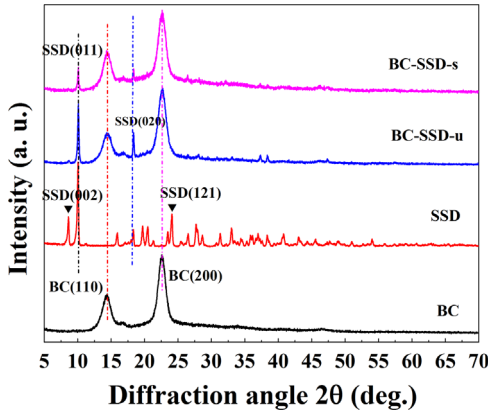

Fig. 3. XRD analysis of BC, SSD, BC–SSD-p and BC–SSD-s membrane.

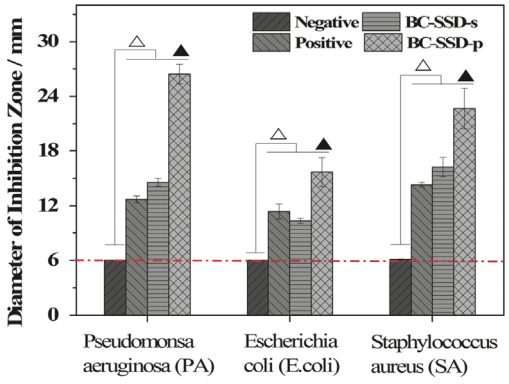

Fig. 4. Diameter of inhibition zone of BC–SSD against *S. aureus*, *E. coli* and *P. aeruginosa* (original diameter of sample was 6.5 mm). Significance: M△ greater than negative control, ▲ greater than positive control. Negative: gauze; positive: a commercial silver-containing dressing.

membrane as the SSD content in BC–SSD-p was much higer than in BC–SSD-s. However, BC–SSD-s composite membrane still exhibited good antibacterial effectiveness with similar inhibition zone against the commercial silver-containing dressing (Coloplast® Ag nonadhesive foam dressing).

The antibacterial ratios of BC–SSD membranes against the three kinds of typical bacteria were tested by the shake flask test method. The bacteriostatic results are shown in Tables 1 and 2. Both of BC–SSD-p and BC–SSD-s composite membranes had effective bacteriostatic rate on *E. coli*, *S. aureus* and *P. aeruginosa*, which were all higher than 99%. The results showed that the antimicrobial effects of BC–SSD-s were similar to the antimicrobial effects of the commercial silver-containing dressing (no significant difference, $P > 0.05$). So, BC–SSD-s membranes could be used as an antimicrobial wound dressing material.

3.4. *In vivo* effect of BC–SSD on partial thickness burn wound healing

BC–SSD-s was selected to test in partial thickness burn wound model since the SSD particles in BC–SSD-p were too large to permeate into the fibrous network of BC completely. The large particles may shed and cause adverse effects on the cell biocompatibility.

3.4.1. Gross examination

Fig. 5 showed the typical macrographs of each wound with different treatments for a period of 4, 7, 10 and 14 days. The healing effect of BC–SSD-s group was obviously greater compared with gauze group in all healing stages. At 4 days, no infection or contraction was observed in the wound of BC–

Table 1
The effect of BC–SSD on proliferation of *Staphylococcus aureus, Pseudomonas aeruginosa, Escherichia coli* ($\pm$ *sd*, $\times$ 102 CFU/cm2).

	Staphylococcus aureus	*Pseudomonas aeruginosa*	*Escherichia coli*
Negative control	98.75 ± 36.99	210.75 ± 4.09	181.63 ± 5.58
Positive control	$0.23 \pm 0.11\Delta$	$0.38 \pm 0.74\Delta$	$0.18 \pm 0.15\Delta$
BC–SSD-s	$0.28 \pm 0.20\Delta$	$0.34 \pm 0.45\Delta$	$0.21 \pm 0.27\Delta$
BC–SSD-p	$0.13 \pm 0.35\Delta$	$0.25 \pm 0.46\Delta$	$0.26 \pm 0.71\Delta$

Significance ($P < 0.05$): Δ greater than negative control. Negative: gauze; positive: a commercial silver-containing dressing.

Table 2
The bacteriostatic rate of BC–SSD to *Escherichia coli*, *Staphylococcus aureus* and *Pseudomonas aeruginosa* (%).

	Staphylococcus aureus	*Pseudomonas aeruginosa*	*Escherichia coli*
Negative control	–	–	–
Positive control	99.77 ± 0.11	99.82 ± 0.35	99.90 ± 0.08
BC–SSD-s	99.72 ± 0.20	99.84 ± 0.21	99.88 ± 0.15
BC–SSD-p	99.87 ± 0.35	99.88 ± 0.22	99.86 ± 0.39

Negative: gauze; positive: a commercial silver-containing dressing.

SSD-s group, while skin was hemorrhagic in the wound of gauze group. At 7 days, the BC–SSD-s group was noted to have scab formation whereas gauze group was inflamed with pus. At 10 days, the scab formation was attained by the gauze group, while the wound of BC–SSD-s group appeared partly healed, leaving scab that was falling off. At 14 days, the majority of the wounds treated with BC–SSD-s composite membrane appeared to be healed. However, the wound of gauze group was still partly swelling and redness.

3.4.2. Wound size reduction

The wound healing rate was calculated as shown in Fig. 5G. After 4 days, the healing rate in BC–SSD-s group was higher than in gauze group with significant difference. At 14 days, the healing rate of the BC–SSD-s group was 92.35%, while the gauze group was only 78.83%, which demonstrated that the BC–SSD-s composite membrane was highly effective in promoting the healing of partial thickness burn wound.

3.4.3. Bacteria reduction of wound surface

As shown in Fig. 5H, there was an increasing trend in bacteria count in the first 4 days. However, the amount of bacteria on the wound surface in BC–SSD-s group was far less than that in gauze group. After 4 days, there was a significant decreasing trend in amount of bacteria for both groups. For BC–SSD-s group, the bacteria count was reduced to below 103 CFU/cm2 after 7 days. However, for the gauze group, 104 CFU/cm2 was still observed at 14 days post-surgery.

3.4.4. Histological examination

The histological examination of the test and control samples is shown in Fig. 5. From the H&E stains, it was noted that BC–SSD-s group had an earlier onset of re-epithelisation compared to control group. At 14 days, both BC–SSD-s group and control group showed the dermis and epidermal layer structure. However, the wound of BC–SSD-s groups was healed, and no epidermal keratinization was observed, while the epidermal tissue slowly extended in the wound of control group. Moreover, the structure observed for control group was comparatively less organized compared to BC–SSD-s group.

The average thickness of fresh epidermal and dermis was calculated by measuring the histological morphology of wound area (Fig. 5(I)). The average epidermal thickness of BC–SSD-s group was 63 μm, while the value for control wound was only about 41 μm. The average thickness of fresh dermis was 149 μm for BC–SSD-s group, while the value was only 95 μm for control group.

Using Masson's trichrome staining, the wound tissue biopsy showed more collagen formed and deposited in the BC–SSD-s group. On day 14, the mature collagen was observed in the dermis in BC–SSD-s group, while immature collagen fibers filled the dermis in the control group.

4. Disscusion

Burn is an evolving and complex injury, the treatment of burn wound can have a considerable influence on the time taken for the wound to heal [30]. An “ideal burn wound dressing” needs the capability of preventing from bacterial penetration [31]. In this study, we demonstrated that, in both *in vitro* and *in vivo* settings, the composite membrane consisting of BC and SSD had the ability to combat high concentrations of bacteria.

We prepared BC–SSD composite membrane by immersing BC into SSD suspension after ultrasonication and centrifugation. In order to impregnate SSD particles in the inner fibers of BC preferably, the particle diameter of SSD should be controlled within an appropriate range. After centrifugation, the supernatantof SSD particles (SSD-s) displayed average particle size of 282.3 nm, respectively with a progressively narrow distribution of particle sizes, just to allow the particles to permeate into the nano-network of BC. BC has a fibrils network and highly porous structure with intrinsic hydrophilicity, which can explain its favorable characteristic of high water holding and tensile strength [18]. The impregnation of SSD into BC had no effects on the overall 3D nano-network of BC, so the outstanding properties of BC were well retained in BC–SSD composite membrane.

As we reported previously [28], BC–SSD composite membrane exhibited great antibacterial effectiveness *in vitro*, which attributed to the impregnation of SSD into BC. In this work, BC–SSD-p composite membrane showed larger inhibition zone than BC–SSD-s composite membrane because of the more SSD content. Even so, BC–SSD-s composite membrane still exhibited well antibacterial effectiveness. SSD particles in BC–SSD-p can hardly permeate deep into the network of BC.

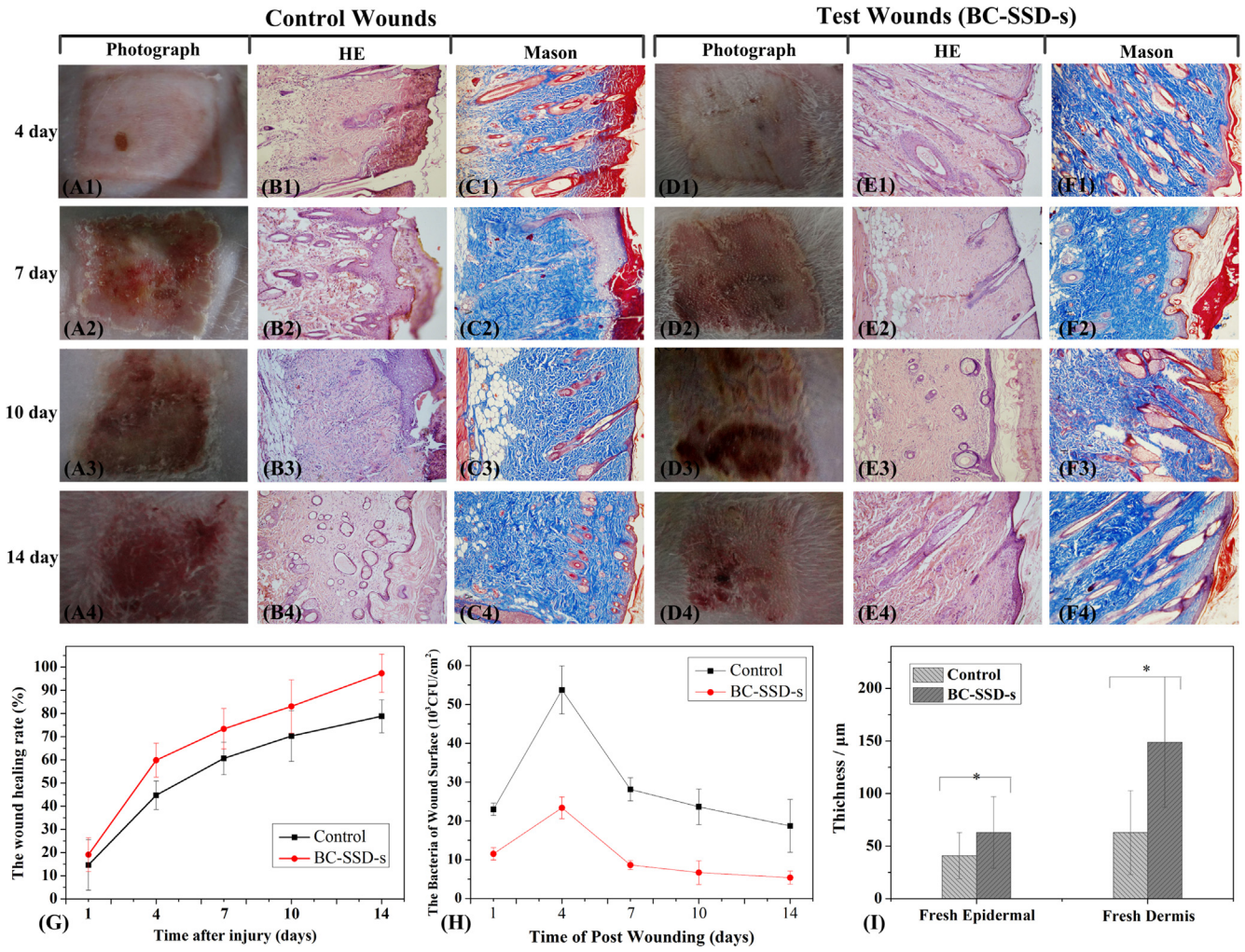

Fig. 5. Representative photographs of macroscopic appearance of 20 mm × 20 mm partial thickness wound excised on rat: control wounds (covered with gauze) at the 4th (A1), 7th (A2), 10th (A3) and 14th (A4) day and test wounds (covered with BC–SSD-s composite membrane) at the 4th (D1), 7th (D2), 10th (D3) and 14th (D4) day. Histology of partial thickness wound: hematoxylin and eosin staining of control wound sections at 4th (B1), 7th (B2), 10th (B3) and 14th (B4) day and test wound sections at 4th (E1), 7th (E2), 10th (E3) and 14th (E4) day; Masson's trichrome staining of control wound sections at 4th (C1), 7th (C2), 10th (C3) and 14th (C4) day and test wound sections at 4th (F1), 7th (F2), 10th (F3) and 14th (F4) day. Wound healing rate (*G*), bacteria of wound surface (*H*) and epidermal and dermal thickness (*I*) of post wounding.

The large SSD particles may shed. Several studies have reported that large amount of SSD have negative side effects and may delay the wound healing process due to the cytotoxic effects [4,32]. Therefore, BC–SSD-s membranes were selected and then evaluated in the rat model.

BC–SSD-s membranes were contrasted with the gauze as control group, so as to evaluate the efficacy of BC–SSD-s to heal the burn wounds in the *in vivo* environment. BC–SSD-s composite membrane can reduce inflammation of burn wound, and accelerate wound closure with a vigorous healing. From the *in vivo* study, the BC–SSD-s composite membrane have showed very good antibacterial property and maintained high antibiotic efficacy up to 14 days. Superficial partial thickness wound can deteriorate into a deeper wound if the wound was infected. It was therefore essential to reduce the invasive infection by minimizing the number of bacteria in the wound. From the H and E stains, it was noted that BC–SSD group had an earlier onset of re-epithelization. Masson's trichrome stain showed that there was more organized collagen in BC–SSD group. These results illustrated that the wound treated with BC–SSD showed a faster healing rate than control. This could be due to the reduction of bacteria in the wound. With the elimination of bacteria, the later stages of wound healing could proceed effectively [32]. For control group, the presence of bacteria and microorganisms could inhibit the wound closure process and wound healing was therefore delayed. This also coincided with the result of the measurement of epidermal and dermal thickness. BC–SSD group showed significantly thicker epidermis and ermis at 14 days compared to the control group. The *in vivo* results indicated that the healing and antibacterial effect in the BC–SSD group was better when compared with the control group.

5. Conclusions

The BC–SSD composite membrane with effective antibacterial and biocompatible abilities applied as a wound dressing

was realized. Well dispersed SSD nanoparticles with narrow size distribution were obtained and the impregnation of SSD into BC has no effect on the overall 3D nanofibril network of BC. By applying the disc diffusion method, BC–SSD composite membrane showed effective antimicrobial activities against *S. aureus*, *P. aeruginosa* and *E. coli*. From the *in vivo* analysis, BC–SSD composite membrane proved effective ability to prevent bacterial infections. The wound treated with BC–SSD showed a faster healing rate and an earlier onset of re-epithelization compared to control according photographic and histological observations. Therefore, BC–SSD composite membranes have been proved to have efficient anti-bacterial performance and benefic influence on the burn wound healing.

Acknowledgments

This study is financially supported by National Natural Science Foundation of China Project (Grant nos. 51273021 and 51473019).

References

[1] A. Nacer Khodja, M. Mahlous, D. Tahtat, S. Benamer, S. Larbi Youcef, H. Chader, L. Mouhoub, M. Sedgelmaci, N. Ammi, M.B. Mansouri, S. Mameri, Burns 39 (2013) 98–104.
[2] H.F. Selig, D.B. Lumenta, M. Giretzlehner, M.G. Jeschke, D. Upton, L. P. Kamolz, Burns 38 (2012) 960–966.
[3] S.A. Jones, P.G. Bowler, M. Walker, D. Parsons, Wound Repair Regen. 12 (2004) 288–294.
[4] H. Hoeksema, D. Vandekerckhove, J. Verbelen, A. Heyneman, S. Monstrey, Burns 39 (2013) 1234–1241.
[5] A.J. Brown, J. Chem. Soc. Trans. 49 (1886) 172–187.
[6] W.C. Lin, C.C. Lien, H.J. Yeh, C.M. Yu, S.h. Hsu, Carbohydr. Polym. (2013) 603–611.
[7] N. Petersen, P. Gatenholm, Appl. Microbiol. Biotechnol. 91 (2011) 1277–1286.
[8] W.K. Czaja, D.J. Young, M. Kawecki, R.M. Brown, Biomacromolecules 8 (2007) 1–12.
[9] M.C.I. Mohd Amin, N. Ahmad, N. Halib, I. Ahmad, Carbohydr. Polym. 88 (2012) 465–473.
[10] H. Zahedmanesh, J. Mackle, A. Sellborn, K. Drotz, A. Bodin, P. Gatenholm, C. Lally, J. Biomed. Mater. Res. B 97 (2011) 105–113.
[11] C.J. Malm, B. Risberg, A. Bodin, H. Bäckdahl, B.R. Johansson, P. Gatenholm, A. Jeppsson, Scand. Cardiovasc. J. 46 (2012) 57–62.
[12] F.K. Andrade, R. Costa, L. Domingues, R. Soares, M. Gama, Acta Biomater. 6 (2010) 4034–4041.
[13] M. Zaborowska, A. Bodin, H. Bäckdahl, J. Popp, A. Goldstein, P. Gatenholm, Acta Biomater. 6 (2010) 2540–2547.
[14] A. Svensson, E. Nicklasson, T. Harrah, B. Panilaitis, D. Kaplan, M. Brittberg, P. Gatenholm, Biomaterials 26 (2005) 419–431.
[15] M. Ul-Islam, T. Khan, W.A. Khattak, J.K. Park, Cellulose 20 (2013) 589–596.
[16] M.H. Kwak, J.E. Kim, J. Go, E.K. Koh, S.H. Song, H.J. Son, H.S. Kim, Y.H. Yun, Y.J. Jung, D.Y. Hwang, Carbohydr. Polym. (2014) 387–398.
[17] L. Fu, Y. Zhang, C. Li, Z. Wu, Q. Zhuo, X. Huang, G. Qiu, P. Zhou, G. Yang, J. Mater. Chem. 22 (2012) 12349–12357.
[18] W. Czaja, A. Krystynowicz, S. Bielecki, R.M. Brown, Biomaterials 27 (2006) 145–151.
[19] G. Yang, J. Xie, Y. Deng, Y. Bian, F. Hong, Carbohydr. Polym. 87 (2012) 2482–2487.
[20] M.C. Robson, Surg. Clin. N. Am. 77 (1997) 637–650.
[21] J. Wu, Y. Zheng, X. Wen, Q. Lin, X. Chen, Z. Wu, Biomed. Mater. 9 (2014) 035005.
[22] T. Maneerung, S. Tokura, R. Rujiravanit, Carbohydr. Polym. 72 (2008) 43–51.
[23] W. Hu, S. Chen, X. Li, S. Shi, W. Shen, X. Zhang, H. Wang, Mater. Sci. Eng. C 29 (2009) 1216–1219.
[24] J. Wu, Y.D. Zheng, W.H. Song, J.B. Luan, X.X. Wen, Z.G. Wu, X. H. Chen, Q. Wang, S.L. Guo, Carbohydr. Polym. 102 (2014) 762–771.
[25] P. Muangman, C. Pundee, S. Opasanon, S. Muangman, Int. Wound J. 7 (2010) 271–276.
[26] B.S. Atiyeh, M. Costagliola, S.N. Hayek, S.A. Dibo, Burns 33 (2007) 139–148.
[27] O. Brandt, M. Mildner, A.E. Egger, M. Groessl, U. Rix, M. Posch, B. K. Keppler, C. Strupp, B. Mueller, G. Stingl, Nanomed.-Nanotechnol. 8 (2012) 478–488.
[28] J.B. Luan, J. Wu, Y.D. Zheng, W.H. Song, G.J. Wang, J. Guo, X. Ding, Biomed. Mater. 7 (2012) 065006.
[29] Y.H. Lin, J.H. Lin, S.F. Peng, C.L. Yeh, W.C. Chen, T.L. Chang, M. J. Liu, C.H. Lai, J. Appl. Polym. Sci. 120 (2011) 1057–1068.
[30] J. Wasiak, H. Cleland, F. Campbell, Cochrane Database Syst. Rev. 4 (2008).
[31] H. Meng, L. Chen, Z. Ye, S. Wang, X. Zhao, J. Biomed. Mater. Res. B 89 (2009) 379–391.
[32] E.Y. Teo, S.Y. Ong, M.S. Chong, Z. Zhang, J. Lu, S. Moochhala, B. Ho, S.H. Teoh, Biomaterials 32 (2011) 279–287.